

Electrospun nanofibers of poly(vinyl alcohol) and chitosan-based emulsions functionalized with cabreuva essential oil

J. Lamarra, M.N. Calienni, S. Rivero, A. Pinotti



PII: S0141-8130(20)33249-9

DOI: <https://doi.org/10.1016/j.ijbiomac.2020.05.096>

Reference: BIOMAC 15579

To appear in: *International Journal of Biological Macromolecules*

Received date: 27 February 2020

Revised date: 3 May 2020

Accepted date: 13 May 2020

Please cite this article as: J. Lamarra, M.N. Calienni, S. Rivero, et al., Electrospun nanofibers of poly(vinyl alcohol) and chitosan-based emulsions functionalized with cabreuva essential oil, *International Journal of Biological Macromolecules* (2020), <https://doi.org/10.1016/j.ijbiomac.2020.05.096>

This is a PDF file of an article that has undergone enhancements after acceptance, such as the addition of a cover page and metadata, and formatting for readability, but it is not yet the definitive version of record. This version will undergo additional copyediting, typesetting and review before it is published in its final form, but we are providing this version to give early visibility of the article. Please note that, during the production process, errors may be discovered which could affect the content, and all legal disclaimers that apply to the journal pertain.

## Electrospun nanofibers of poly(vinyl alcohol) and chitosan-based emulsions functionalized with cabreuva essential oil

J. Lamarra<sup>a,b</sup>, M.N. Calienni<sup>c</sup>, S. Rivero<sup>a,b</sup>, A. Pinotti<sup>a,d,\*</sup>

<sup>a</sup> Centro de Investigación y Desarrollo en Criotecnología de Alimentos (CCT-CONICET La Plata), 47 and 116, La Plata 1900, Argentina

<sup>b</sup> Facultad de Ciencias Exactas, UNLP, Argentina

<sup>c</sup> Laboratorio de Bio-Nanotecnología-GBEyB (Imbice, CCT-La Plata, CONICET). Departamento de Ciencia y Tecnología, Universidad Nacional de Quilmes, Bernal (1876), Argentina

<sup>d</sup> Facultad de Ingeniería, UNLP, Argentina

### Abstract

Among the essential oils (EOs), the cabreuva essential oil extracted from the wood of *Myrocarpus fastigiatus*, is a promising compound for potential applications in the field of pharmaceuticals and food packaging. To overcome the low solubility of cabreuva EO and to protect it, a two-step process, emulsion formation compound by chitosan, SDS, and PVA, and subsequent ionic crosslinking with sodium citrate, was proposed. The formulation containing 0.75% of chitosan and 1% of SDS proved to be the most stable. An alternative to produce nanostructures and encapsulate the EO is the fiber formation through the electrospinning method. The system composed by a PVA solution assembled with crosslinked emulsions modified the viscosity, influencing the morphology of the obtained nanofibers. The advantage of the electrospun nanofibers was their ability to be an effective carrier of the cabreuva EO and the capacity of controlling the compound release that proved an effective activity against broad spectra of micro-organisms (*Candida albicans*, *E. coli*, *S. aureus*, and *S. epidermidis*).

The Gallagher-Corrigan model, used to fit the release profiles of matrices in contact with increasing ethanol proportion from 25:75 to 50:50 showed higher  $K_b$  in relation to  $k$  suggesting that the polymer swelling played an increasingly prominent role in the EO delivery. The developed nanostructures would be materials with potential applications in the biomedical field.

Key words: electrospinning, cabreuva essential oil, chitosan, controlled release

Corresponding author: [acaimpronta@hotmail.com](mailto:acaimpronta@hotmail.com) (A. Pinotti)

## 1. Introduction

In recent years, electrospun nanofibrous scaffolds used for tissue engineering and controlled drug delivery vehicle [1] have been considered an important group of one-dimensional nanostructures because of their unique properties such as high surface area, high porosity, and their high safety in comparison with other nanomaterials [2,3]. Compared to the traditional encapsulation techniques, the key advantage of the electrospinning process is the absence of heat, which is important for preserving the structure and achieving high encapsulation efficacy of the bioactive substances upon processing and storage [4].

The architecture of these nanostructures makes them appropriate for topical applications in which a network composed of nanofibers is placed directly on healthy skin, wounds or burns to release the active compound [5].

In particular, electrospinning is interesting for the development of antimicrobial materials by either the use of inherently antimicrobial polymers or the nanoencapsulation of antimicrobial substances [6]. Polyvinyl alcohol (PVA) is one of the most common polymers used to attain nanofibers. Ranjbar-Mohammadi *et al.* [7] studied the properties of fibers based on tragacanth gum and PVA functionalized with curcumin produced by electrospinning, obtaining satisfactory results of cell adhesion. On the other hand, Puttamayutanon *et al.* [8] developed active fibers of PVA functionalized with Thai honey with antioxidant and antimicrobial properties.

On the other hand, essential oils (EOs) have been investigated for their potential applications in the field of pharmaceuticals and food packaging. Among the variety of essential oils, the cabreuva essential oil is extracted from the wood of *Myrcarpus fastigiatus*. This EO has been used by natives for the treatment of diverse affections like asthma, rheumatism, extern and intern burns, tuberculosis, bronchitis, wounds, among other conditions [9].

EOs are frequently unstable and can be easily degraded in stressful situations because of the presence of oxygen, temperature and light [10]. In this sense, the nanoencapsulation is characterized by enhancing the bioavailability of the active compound and protecting them

against the degradation by direct exposure to severe environments or processing effects reducing their loss of activity [11].

Chitosan, a natural copolymer of N-acetyl-d-glucosamine and d-glucosamine units, is one of the polysaccharides potentially most suitable as carriers for a large number of active compounds [12,13]. In this sense, to overcome the problem of the low solubility of cabreuva and to protect it, a two-step process, emulsion formation based on chitosan and PVA and ionic gelation with sodium citrate was used.

A strategy to modulate the release of active compounds has been developed through the use of nanodelivery systems to carry essential oils. The inclusion of EO-loaded chitosan nanoparticles in an electrospun mat represents a technical innovation and has potential to be utilized as both a tissue engineering scaffold and a controllable drug encapsulation [2,14]

Notwithstanding the great amount of research to date, the nanoencapsulation of cabreuva essential oil as a compound with potential use in the design of materials for controlled release has not yet been studied. In the present study, we aimed to design a model scaffold with electrospinning technique that allows the diffusion of encapsulated essential oil.

In this context, the synthesized crosslinked nanoemulsions were analyzed from a stability point of view. Once the crosslinked emulsions were incorporated into the PVA matrix, the rheological behavior was determined to ensure an efficient electrospinning process. The morphology of the fibers was examined through scanning electron microscopy (SEM) and confocal laser scanning microscopy (CLSM). The thermal behavior and microstructural properties of the formed nanostructures were analyzed. Finally, the antibacterial capacity of the scaffolds was analyzed, as well as their ability to modulate the controlled release of essential oil in different media.

## 2. Materials and methods

### 2.1 Materials

Chitosan from crab shells (deacetylation degree of 85% and molecular weight of  $3.2 \times 10^5$  Da) was purchased by Polymar Ciência e Nutrição (Fortaleza, Brazil). Polyvinyl alcohol (PVA) was supplied by DuPont (USA) with a hydrolysis degree of 86-89% and a molecular weight in the range of 50 to 55 kDa, sodium dodecyl sulfate (Cicarelli, Argentina) was used as a surfactant agent, the sodium citrate (Cicarelli, Argentina) as a crosslinking agent, and cabreuva essential oil, supplied by Esencias del Bosque (La Plata, Argentina), as an active agent.

### 2.2 Methods

#### 2.2.1 Formulation of nanoemulsions

EO-loaded chitosan nanoparticles were prepared by a two-step emulsion-ionic gelation technique. CH solution 0.75% (w/v) was solubilized in 0.75% (v/v) acetic acid solution for 24 h, while PVA solution was formed dissolving the polymer in water at 90°C for 3h.

In the first step, the formulation of oil in water emulsion (O/W) was performed following a similar protocol described by Li *et al.* [15]. To analyze the effect of chitosan and SDS concentrations, 4 formulations were evaluated as shown in Table 1.

Concentrations of 0.5 y  $1 \text{ g l}^{-1}$  of SDS were solubilized in distilled water. Then, the chitosan solution prepared at a concentration of 0.75% w/v and the PVA solution (0.75% w/v) were incorporated. After that, the cabreuva essential oil was added by dripping while the system was homogenized with an Ultraturrax T-25 (Janke and Kunkel, IKA-Labortechnik, Germany) at 21,000 rpm for 10 minutes. Finally, to decrease the droplet size and increase the system stability, the emulsion was treated with ultrasound using Sonics VCX-750 ultrasonic processors (Vibra Cell, USA) at a power of 750 W and 50% amplitude for 5 minutes.

In the second step, the crosslinking of the emulsions was carried out using sodium citrate at a concentration of 0.125 % (w/v) through the ionic gelation technique (CE).

### 2.2.2 Analysis of the emulsions

The hydrodynamic diameter of the nanoparticles was determined by light scattering with a Malvern Mastersizer 2000E particle analyzer with a Hydro 2000MU dispersion system (Malvern Instruments Ltd., Worcestershire, United Kingdom). On the other hand, the zeta potential values (PZ) of the emulsions were performed using Horiba Scientific Equipment-Model SZ-100Z (Horiba, Ltd.).

The global stability of the emulsions was carried out by light scattering with a vertical scan analyzer (QuickScan, Beckman Coulter, Fullerton, USA) at room temperature following a procedure described by Lamarra *et al.* [16]. Briefly, the formed emulsions were placed in cylindrical test tubes and scanned from the bottom at the tip of the tube with a monochromatic light source ( $\lambda = 800$  nm) acquiring the *BackScattering* profile at different days (between 10 and 13 days).

Likewise, the morphology of the emulsions obtained was characterized through transmission electron microscopy (TEM) using a microscope JEM 1200EX II Jeol (Japan) equipped with a digital camera (ES500W Erlangshen CCD). A drop of the emulsion placed in a pretreated copper grid was coated with an amorphous thin carbon film.

### 2.2.3 Formulation of solutions

PVA solutions prepared at different concentrations: 12, 14 and 16% w/v and were solubilized at 90°C for 3 hours.

Once the concentration of PVA required to obtain continuous and regular fibers was selected through SEM, the polymeric solution was functionalized assembling cabreuva EO-loaded chitosan nanoparticles cross-linked with sodium citrate. For this purpose, a PVA solution with the highest concentration (16% w/v) was assembled with the emulsions in different proportions until reaching a final concentration that could be electrospun without failures. In this sense, the PVA: crosslinked emulsion ratio selected was 3:1 (on weight).

#### *2.2.4 Rheological properties of the solutions*

To establish and to describe the flow behavior of the polymeric solutions, a Haake RheoStress600 rheometer (Germany) was used. A dish-plate sensor system with rough surfaces and a gap between the plates of 1 mm were selected. From the rotational tests, the shear stress flow curves were obtained as a function of the shear rate.

#### *2.2.5 Nanofibers forming by electrospinning*

The experimental equipment used consists of four components: a polymeric solution reservoir (PVA solution with the emulsion assembled), an infusion pump with syringe PC11UB APEMA (Argentina) that allowed supplying a flow in the range between 0.3 and 1 ml h<sup>-1</sup> of polymer solution, a high voltage power supply (up to 30 kV) and a stainless steel collector system. Based on previous tests, a flow of 0.4 ml h<sup>-1</sup>, a voltage of 24 kV, a collector-needle distance of 27 cm and a distance between the electrodes of 29 cm, keeping the horizontal electrospinning setup were selected. The nanofibers were collected for 5 hours until obtaining a film with a thickness capable of being unmolded from the collector plate.

From now on, the nomenclature used for the nanofibers will be PVA<sub>E</sub> for electrospun PVA 14% used as control and (PVA+CE)<sub>E</sub> for electrospun nanostructures attained from the suspension of PVA and the crosslinked emulsion.

#### *2.2.6 Morphological analysis of nanostructures by microscopy*

The morphological analysis of the nanofibers was carried out through scanning electron microscopy (SEM) by using of FEI model Quanta 200 microscope (The Netherlands). Specimens were examined at an acceleration voltage of 15 kV. The diameter of the fibers was calculated by using Fiji program (Image J, NIH, USA).

Likewise, in the cases of nanostructures functionalized with cabreuva essential oil, the use of the confocal scanning laser microscopy (Olympus FV300 with an increase of 20X and DAPI filter) technique was used to visualize the distribution of the cabreuva essential oil in the mat.

### 2.2.7 Thermal and microstructure studies of nanostructures

DSC analyses were carried out a heating rate of  $10^{\circ}\text{C min}^{-1}$  by using a DSC model Q100 controlled coupled with a TA 5000 module (TA Instruments, New Castle, Delaware, USA) according to the procedure described by Villarruel *et al.* [17]. On the other hand, TGA analysis was carried out in aluminum capsules under a nitrogen atmosphere (flow rate  $30\text{ ml min}^{-1}$ ) with a Shimadzu DTG-60 (Japan) equipment. The heating ramp was conducted at  $10^{\circ}\text{C min}^{-1}$  from room temperature to  $600^{\circ}\text{C}$ .

To analyze the microstructure of the electrospun fibers, the X-ray diffraction technique was employed using a XRD Philips PW3710, X'Pert Pro P Analytical ModelPW3040/60 (Almelo, The Netherlands) at room temperature.

Fourier transforms infrared spectroscopy equipment (Nicolet, iS10 ThermoScientific, Madison, USA) was used in the attenuated total reflectance mode (Smart iTX accessory). The data recorded in the range of  $400\text{-}4000\text{ cm}^{-1}$  by the accumulation of 32 scans with a resolution of  $4\text{ cm}^{-1}$  were analyzed using Omnic 8 software (ThermoScientific).

### 2.2.8 Antimicrobial capacity

Media plates with Mueller-Hinton agar were previously inoculated by dispersion on the entire surface with  $100\text{ }\mu\text{L}$  of bacterial suspension of *Staphylococcus aureus*, *Staphylococcus epidermidis*, *Escherichia coli*, and *Candida albicans* obtaining a concentration of microorganisms of the order of  $10^7\text{-}10^8\text{ CFU ml}^{-1}$ . The preparation of the inocula and the antimicrobial capacity of the active mats were determined by using the agar diffusion method according to Villarruel *et al.* [17]. Discs of mats ( $1.5\text{ cm}$  in diameter) were used to estimate the inhibition zones after 24 and 48 hours of contact with the media using specific image analysis software (Image J, NIH, USA).

### 2.2.9 Release of cabreuva EO

To evaluate the controlled release kinetics of the cabreuva essential oil, squares of  $2.5\times 2.5\text{ cm}^2$  of the electrospun nanofibers were immersed in  $50\text{ ml}$  of ethanol: water mixture in different ratios ( $75:25$ ,  $50:50$ ;  $25:75$ ) to modify the affinity of the EO with the solvent. Furthermore, we



assayed different ethanol: water ratios in order to analyze the influence of the affinity of the active compound with the solvent on the release profile. Samples were withdrawn at different times and placed into black 96-well plates. The fluorescence emission signal was measured in a microplate reader exciting at 340 nm and emitting at 420 nm (SYNERGY HT-SIAFRT, Biotek Instruments, Vermont, USA).

### 2.3 Statistical analysis

Infostat v2009 software (Córdoba, Argentina) was used for all statistical analysis. Analysis of variance (ANOVA), linear and non-linear regressions and Fisher LSD mean comparison test was applied. The significance level used was 0.05.

## 3. Results and discussion

### 3.1 Stability of emulsions

The nanoemulsions were prepared by an ionic crosslinking reaction between the protonated amino groups of the CH and the groups  $\text{COO}^-$  of the sodium citrate. The electrostatic interaction allowed the encapsulation of an amount of EOs within the matrix of CH [16].

The selection of the emulsion to be assembled with the PVA solution was achieved by-means of physical stability studies. A variant is to use polymers that contain specific groups with a high affinity for oil. Poly(vinyl alcohol) (PVA) is a polymer obtained by partial hydrolysis of polyvinyl acetate (PVAc) that leaves some residual vinyl acetate groups. These hydrophobic acetate groups give the molecule its amphipathic character, a condition required to form an emulsion [18].

Zeta potential values of the formulated emulsions are summarized in Table 1. The change in ZP values with the addition of chitosan would indicate mainly ionic interactions between the SDS and amino groups of CH present in the continuous phase of the emulsion [19]. Likewise, the increase of ZP until reaching high positive values confirmed the presence of chitosan forming part of the emulsion, as well as free in the system [20].

It is pertinent to clarify that chitosan is a cationic polyelectrolyte that can be assembled forming a layer or interfacial film on the oil drop coated with SDS anion [13].

In the formulations without chitosan, a creaming process was visualized (Figure 1a and c) since the droplets tend to migrate towards the upper part resulting in a separation of phases [21]. The presence of chitosan improved the stability of the emulsions thus there was no evident growth of the droplets or migration of the emulsion (Figure 1b and d).

There was no phenomenon of creaming, although there was a slight decrease in the value of BS in accordance with Julio *et al.* [21]. The authors assigned this behavior to increase in the viscosity of the continuous phase, thus reducing the mobility of the oil droplets combined with the electrostatic repulsion between them. Other authors sustain that the combination of a surfactant with a polyelectrolyte induces a significant decrease of the superficial tension due to the adsorption of the polymer in the interface leading to prevent coalescence of the droplets promoting greater system stability [22]. SDS molecules reduce the interfacial tension and it is able to form a protective layer on the oil droplets causing the repulsion between them [23].

On the other hand, the emulsion  $E_1$  (SDS  $0.5 \text{ g l}^{-1}$ ) presented the largest-droplet size meanwhile the addition of chitosan shifts the distribution to minor sizes  $E_2$  (CH/ SDS  $0.5 \text{ g l}^{-1}$ ). A similar trend was observed for  $E_3$  (SDS  $1 \text{ g l}^{-1}$ ) and  $E_4$  (CH/ SDS  $1 \text{ g l}^{-1}$ ). Furthermore, the inclusion of a greater amount of SDS in the formulation that contained chitosan led to a greater reduction in size, whereas the addition of sodium citrate (0.125 % w/ v) as a crosslinker agent of the emulsion did not influence the profiles obtained for  $E_4$  (data not shown). These results correlated with the trend observed for the ZP, as well as with the emulsion stability analysis, reinforcing the hypothesis of a decrease or delay in the coalescence process due to the presence of CH and SDS. Hou *et al.* [24] informed analogous results working on emulsions of  $\beta$ -carotenes stabilized with soluble soy polysaccharides and chitosan. According to Aoki *et al.* [25], the presence of chitosan in emulsions (O/W) prepared with corn oil and SDS as a surfactant agent induces an increase in the droplet size and favors the bridging flocculation. An opposite effect was achieved after the application of ultrasound to the emulsions.

The micrographs recorded by TEM confirmed the results previously described, showing sizes in the range 275-370 nm (Figure 2b-e).

In all images, the presence of a layer of SDS as described by Chatterjee *et al.* [20] can be observed. Figure 2b-e shows the changes experienced by the emulsion after the crosslinking caused by the addition of citrate sodium confirming the ionic interaction.

Table 1 summarizes the variation of values of *BackScattering* (BS) in the tube region between 10 and 15 mm after 7 days of storage [26]. Confirming the behavior observed in the *BackScattering* profiles. The emulsion prepared with the lowest amount of chitosan and without SDS content showed a significant change ( $p < 0.05$ ) compared to the initial value, while the addition of chitosan ( $0.5 \text{ g l}^{-1}$ ) led to a less pronounced reduction, although a value of 15% indicates the occurrence of the creaming process [26]. The emulsion without CH such as E<sub>3</sub> resulted in large variations in the values of *BackScattering*. Table 1 reveals that the emulsion E<sub>4</sub> presented a reduction by 6% after 7 days, which indicated that there was no mechanism of destabilization [26].

Pursuant to these results, it was proposed the use of the crosslinked emulsion with greater stability. Therefore, to obtain the nanostructures by electrospinning process, the emulsion selected to be assembled with the PVA solution was that formulated with a surfactant concentration of  $1 \text{ g l}^{-1}$  and sodium citrate 0.125 % (w/v).

### 3.2 Rheological behavior of solutions

The adequate selection of the process parameters allows controlling the fiber diameter and its characteristics. The concentration and the viscosity of polymer solution are factors that determine the size and morphology of the fiber.

The rheological behavior was adjusted through the Ostwald-de Waele model:

$$\tau = k_v \gamma^{n_v} \quad \text{Eq.1}$$

where,  $\tau$  is the shear stress,  $\gamma$  is the shear rate,  $k_v$  is the consistency index, and  $n_v$  the flow behavior index. The apparent viscosity ( $\eta$ ) was determined at  $500 \text{ s}^{-1}$ . The estimated rheological parameters are presented in Table 2.

The individual emulsions presented a Newtonian behavior. Polymeric solutions with and without emulsion functionalized with cabreuva essential oil exhibited values of the consistency index lower than 1, reflecting a non-Newtonian behavior consistent with a pseudoplastic flow,

which is required for the electrospinning process [27]. In this case, the existence of a significant difference in the value of  $n_v$  between the PVA solution (14%) and (PVA+CE) suspension was observed. After the assembling of the emulsion with the polymer solution, the value of  $n_v$  became closer to 1, because the viscosity of the emulsion was 0.0093 Pa.s. This result was similar to that obtained by Pal *et al.* [27] working on polycaprolactone emulsions dispersed in a continuous phase of PVA.

Table 2 shows a decrease in the apparent viscosity of the solution containing the emulsion due to the decrease in PVA concentration leading to a lower capacity to form fibers. Phachamud & Phiriyawirut [28] informed that an increase in viscosity with the increase in polymer concentration improves the electrospun fiber formation. Similar behavior was reported by Pangon *et al.* [29] for blends of chitosan and PVA. The decrease in the viscosity with the increase of CH proportion was explained considering the higher polymer-solvent interactions due to the presence of chitosan.

### 3.3 Fiber morphology

Figure 3a and b show the micrographs of electrospun fibers obtained using PVA solutions prepared at 12% and 14%, respectively. As can be seen in Figure 3, the PVA 12% sample presented the appearance of beads in its structure, while the PVA 14% sample showed a uniform structure free of beads. This phenomenon can be explained by considering the direct relationship between polymer concentration and the viscosity of the polymer solution [28]. A smaller diameter of the fibers in the sample PVA 12% could also be observed due to the lower viscosity of the polymer solution.

Since the formation of homogeneous and continuous fibers without the presence of beads in their structure is desirable, the concentration of 14% (PVA<sub>E</sub>) was selected to obtain the control matrices.

Figure 3c depicts the SEM micrograph of (PVA+CE)<sub>E</sub> sample. The blend of the polymer with the emulsion led to a system with lower viscosity, with the formation of beads interrupting the network of PVA fibers. Similar results were found by Puttamayutanon *et al.* [8] working on PVA matrices loaded with honey. Another aspect to be considered is the presence of chitosan as a

component of the emulsion, which generates a modification in the electrospinning process. Talebian *et al.* [30] explained the influence of the CH concentration on the morphological properties of the nanostructures based on PVA. These authors found that a proportion of chitosan higher than 50% led to the formation of beads in the obtained fibers.

Figure 3a, b and c depicts the histograms showing the distribution of fiber sizes for each of the formulations obtained through the analysis of the micrographs obtained by SEM.

The sample PVA<sub>12</sub> presented a size fiber distribution center mostly at 150 nm (Figure 3 a). The higher concentration of polymer (PVA) the greater proportion of fibers with diameters centered at 200 nm was observed (Figure 3 b). On the other hand, the inclusion of the emulsion in the system caused a reduction in the population of fibers with sizes greater than 200 nm (Figure 3c). Similar results were observed by Rieger & Schiffman [31] working on fibers based on chitosan and polyethylene oxide functionalized with cinnamaldehyde.

Likewise, the micrographs obtained by CLSM exhibited a uniform distribution of cabreuva essential oil because of the inherent fluorescence of the active compound (Figure 4). López-Córdoba *et al.* [32] reported similar results working on electrospun PVA matrices loaded with tetracycline hydrochloride.

### 3.4 XRD analysis

The X-ray diffraction patterns of the matrices collected after the electrospinning process are shown in Figure 5.

As was studied in previous work [33], PVA exhibited a typical peak at  $2\theta = 19^\circ$  associated with the plane (101) of the semicrystalline structure due to the strong hydrogen bridge-type interactions established between the polymer chains. However, the polymer processed by electrospinning decreased the intensity of the diffraction peak, a phenomenon that correlated with the decrease in the crystallinity of the PVA [10]. A similar trend was observed by Basha *et al.* [34] and Enayati *et al.* [35] who reported a significant decrease of PVA crystallinity as a consequence of the electrospinning process. Pangon *et al.* [29] found similar results working on blends of chitosan and PVA cross-linked with different acids. Likewise, Krstić *et al.* [36] suggested that this phenomenon can be explained taking into account that the orientation of

the molecules in the direction of the fibers has less time to align with each other, generating a less favorable packaging. Additionally, these authors remarked that for being a semicrystalline polymer, the stretching of the chains subjected to high elongation rates does not provide enough time to form a lamellar crystal structure, which results in a lower degree of crystallinity.

On the other hand, the addition of emulsion to the PVA did not modify the diffraction pattern compare to the electrospun PVA spectra but generated an increase in the CD. On the other hand, Enayati *et al.* [35] informed a satisfactory correlation between CD determined through DSC and XRD.

### 3.5 Thermal analysis

Figure 6a shows the thermograms obtained by TGA of the PVA<sub>E</sub> matrix observing three loss mass stages: the first event was associated to water loss presents in the matrix (near to 80°C), the second one attributed to chain decomposition (200-350°C), and the third stage was related to the degradation of by-products (350-480°C) [32,37]. From de curves, it was not detected loss mass corresponding to essential oil evaporation (Figure 6b). This result corroborated that the electrospinning process maintained the structural configuration in which the essential oil was initially confined.

As can be seen in no differences were observed in the glass transition temperature ( $T_g$ ) between the samples of PVA<sub>E</sub> and (PVA+CE)<sub>E</sub> produced by electrospinning. These results confirmed the compatibility between the PVA matrix and the emulsion. In this way, Pal *et al.* [27] reported similar results working on PVA and poly ( $\epsilon$ -caprolactone) composite emulsions processed by electrospinning.

According to Olabisi *et al.* [38], a change in the crystalline structure can be the result of polymer-polymer interactions established in the amorphous phase. In accordance with Enayati *et al.* [35], the diminution in the crystallinity degree due to the formation of fibers by electrospinning was explained assuming the short time available to solvent evaporation. The changes in CD after the addition of emulsion were probably the result of a hetero-nucleation.

Bearing in mind that after electrospinning processing there was a rearrangement of the structure of the polymer chains, a significant shift ( $p < 0.05$ ) of the endothermic event assigned

to the melting of the crystalline phase towards lower temperatures was observed. However, the addition of emulsions did not generate statistically significant changes ( $p>0.05$ ) in this transition. These results were concordant with the findings observed by means of the XRD technique.

### 3.6 ATR-FTIR

Deng *et al.* [39] found that structural changes generated by the electrospinning process can be detected through ATR-FTIR. Figure 7 shows the FTIR spectra of cabreuva EO, samples of PVA<sub>E</sub> as well as (PVA+CE)<sub>E</sub>. All samples gave a strong band centered at about  $3288\text{ cm}^{-1}$  confirming the presence of both, strong intra- and intermolecular hydrogen bonding and the free OH groups. The characteristic bands of PVA were displayed in both, PVA<sub>E</sub> and (PVA+CE)<sub>E</sub> ATR-FTIR spectra. The shift of the band located at  $3288\text{ cm}^{-1}$  toward  $3270\text{ cm}^{-1}$  would result from the formation of hydrogen bonds between amino groups or hydroxyl groups in chitosan and hydroxyl groups in PVA [40].

Both, the CH<sub>2</sub> symmetric and antisymmetric stretching vibration bands were located at  $2910$  and  $2855\text{ cm}^{-1}$ . Other stretching vibrational bands appeared at  $1660$  and  $1565\text{ cm}^{-1}$  for C=O and C=C groups. At  $1141\text{ cm}^{-1}$  a peak, assigned as C–C and C–O–C stretching vibrations correlated to the polymer crystallinity was not influenced by the presence of the emulsion and remained unchanged [17]. The observation of this absorption band is a signal of the semicrystalline character of the PVA.

Some peaks located at  $1744$ ,  $1240$  and  $1086\text{ cm}^{-1}$  associated with the stretching vibration of functional groups carbonyl (C=O), acetyl (O-C-O) and acetal (-C-O-), respectively, were observed. According to Zahedi *et al* [41], these peaks correspond to residual acetate groups and are a consequence of the incomplete hydrolysis degree of PVA chains (86-89 %).

The slight modifications observed in the regions  $3000-2800\text{ cm}^{-1}$  and  $950-850\text{ cm}^{-1}$  suggest the chemical interaction between PVA-EO and could be attributed to the presence of cabreuva EO embedded into the PVA matrix. The encapsulation of the cabreuva EO was supported by the ATR-FTIR spectra since the PVA chemical structures remained broadly unchanged.

### 3.7 Antimicrobial capacity of electrospun fibers

The antimicrobial capacity of fibrous nanostructures (PVA+CE)<sub>E</sub> was evaluated against *Candida albicans*, *E. coli*, *S. aureus*, and *S. epidermidis*. The results are summarized in Table 3.

It was observed that the fibers formed exhibited antibacterial capacity against the microorganisms tested, which could be due to the presence of the essential oil and chitosan in the samples and to the diffusion of the compound once it had contact with the culture medium. The mat obtained due to PVA<sub>E</sub> fiber deposition did not present antibacterial activity against the microorganism studied. Similar results were observed by López-Córdoba *et al.* [32] for tests carried out against *E. coli* and *S. aureus*.

The antibacterial activity against Gram-positive bacteria such as *S. aureus* and *S. epidermidis* of the functionalized fibrous nanostructures was found to be greater than that observed for *E. coli*. This phenomenon was attributed mainly to the superficial characteristics of the cells and to the structural differences of the cell walls of bacteria. This result was also confirmed by Adeli *et al.* [41] working on fibrous matrices composite with chitosan, starch, and PVA nanostructured by electrospinning. These authors observed greater antibacterial capacity against *S. aureus* compared to *E. coli*.

### 3.8 Cabreuva essential oil release

As was described, the release of cabreuva EO from PVA matrices was performed after the immersion in the release medium. Different ethanol: water ratios were assayed in order to analyze the influence of the affinity of the active compound for the solvent on the release profile. To modify the polarity of the solvent (distilled water), we include alcohol in the formulation as the release media. According to Sanchez *et al.* [42] (2020) the ethanol is added to help release the essential oil more uniformly.

The experimental data were fitted to different kinetic models to determine the mechanism controlling the cabreuva essential oil release kinetics from the electrospun matrices.

The semiempirical equation proposed by Korsmeyer-Peppas [43], derived from Fick's law, was used to describe the release kinetics of EO from polymeric nanostructure.



$$\frac{M_t}{M_\infty} = F_T = k \times t^n \quad \text{Eq. 2}$$

where,

$M_t/M_\infty$  is the fraction released of active compound at time  $t$ ,  $k$  is the transport constant (dimension of  $\text{time}^{-1}$ ) and  $n$  is a parameter representative of the mechanism of transference of the active agent.

The parameter  $k$  indicates the constant active compounds transport that can be seen intuitively as directly proportional to the active compound release kinetic from the nanostructures. Bearing in mind this fact, higher  $k$  indicated faster cabreuva essential oil release as was the case of matrices that were in contact with the 75:25 medium. On the contrary, a lower value of  $k$  indicated a slower transport kinetic (Table 4).

The exponent  $n$  was near 0.4 for the release in ethanol: water 25:75 medium (Table 4) indicating that a pseudo-Fickian diffusion controlled the EO release pattern. Since the diffusion exponent obtained was  $n = 0.6$  in 50:50 medium, the release of the active compound would be governed by a mechanism combining a diffusion type Fickian and swelling process confirming an anomalous mechanism in this latter case.

In the case of 75:25 medium, the mechanism interprets that the relaxation of the matrix occurs when the water control the speed of release ( $n = 1$ ) due to a swelling process. The model is non-Fickian (Case II) in which the EO delivery rate corresponds to zero-order release kinetics and the mechanism involved is the swelling or relaxation of polymeric chains [43].

Similar results were found by Moydeen *et al.* [44] working on electrospun poly(vinyl alcohol)/dextran nanofibers as a carrier for ciprofloxacin (Cipro) as a model drug delivery.

Figure 8 shows the percentage of cabreuva essential oil released in media with different ethanol: water ratios. At the initial phase, electrospun nanostructures exhibited a marked burst release, and then the curve tended to a plateau or a gradual release. The increase in the ethanol content in the medium caused an increase in the amount of active component released intensifying the burst effect [45], which was demonstrated by the values of the constant  $K_b$

(Table 4). This fact may be due to an increase in the affinity of the essential oil for the medium. Similar results were observed by Villasante *et al.* [46] working with films of poly (lactic) acid charged with  $\alpha$ -Tocopherol, a hydrophobic compound.

In ethanol: water 75:25 medium, a rapid *burst* stage occurred after 6 minutes in which 85% of the active product was released (Figure 8). This result was similar to that observed by Estevez-Areco *et al.* [45] who reported a rapid release of a *Rosemary* ethanolic extract contained in PVA fibers obtained by electrospinning. Souza *et al.* [47] also observed a similar result working with polylactic acid nanofibers (PLA) used to encapsulate linalool by synthesizing fibers with varying amounts of terpene, reporting that the amount of linalool on the surface results in the release of more than 80% in just 30 minutes.

The release of EO in a medium richer in water was slower; therefore, the rate of EO release depended on the composition of the media in which the diffusion was carried out.

The experimental data were fit by means of the Gallagher-Corrigan model

$$FT = Fb(1 - e^{-Kbt}) + (1 - Fb) \frac{e^{kt-kt_{max}}}{1 + e^{kt-kt_{max}}} \quad \text{Eq. 3}$$

where,  $K_b$  is the burst rate constant,  $F_b$  the fraction of the active compound released in the burst phase,  $t_{max}$  the time for maximum rate and  $k$  is the rate constant of the polymer degradation phase.

The release can also be described by other models known as the Gompertz [48], Weibull, and Higuchi [49] models as follows:

$$\frac{M_t}{M_\infty} = \exp[-a \times \exp(b \times \log t)] \quad \text{Eq.4}$$

where,  $M_t/M_\infty$  is the percent of active agent release at time  $t$ ,  $a$  parameter determines the undissolved proportion at  $t=1$  described as a location or scale parameter,  $b$  dissolution rate per unit of time describes a shape parameter.

$$\frac{M_t}{M_\infty} = 1 - \exp\left[-\frac{(t - T_i)^b}{a}\right] \quad \text{Eq.5}$$

where,  $a$  is a parameter relative to the time process,  $T_i$  is the lag time, in most cases zero, and  $b$ , the shape parameter and characterizes the release curve shape.

On the other hand, according to da Costa et al. [50] modifications on release profile are induced by the geometry of matrix and diffusion of active compound along cylindrical structures is conveniently described by Weibull model.

$$\frac{M_t}{M_\infty} = k_H \times t^{1/2} \quad \text{Eq.6}$$

where,  $k_H$  is the Higuchi dissolution constant. The Higuchi model uses pseudo-steady-state assumptions to describe the release kinetics of the active compound from a porous matrix based on Fick's law [44].

The properties of the polymeric solution and its interaction with bioactive compounds influence the distribution of the latter compound in the nanofibers and therefore its release profile [51]. The initial step, related to the *burst*, was ascribed to the surface-loaded cabreuva EO which had a weak bound with the nanofiber surface, hence it had a high diffusion trend. The second step of release could be attributed to the diffusion of the EO molecules from the *bulk* of the nanofibers.

As is evident from Table 4, the Gallagher-Corrigan model achieved a better fitting in relation to Gompertz and Weibull models. Based on Higuchi model, the drug release occurs by diffusion within the delivery system. In this case, the cumulative amount of the drug released is proportional to the  $t^{1/2}$  [44]. Given that Higuchi model considers that the drug release occurs by diffusion, the results supported that the higher the ethanol proportion in the release medium, the farther the behavior of the system drifted from a Fickian model.

The fitting parameters for release profiles of matrices in contact with increasing ethanol proportion from 25:75 to 75:25 showed higher  $K_b$  concerning  $k$  (Table 4) suggesting that the polymer swelling played an increasingly prominent role in the EO delivery.

Two opposite effects were observed because of the presence of ethanol and water. The increase in the ethanol proportion led to a greater solubilization of the cabreuva essential oil and a sudden release in the burst step with  $k_b \gg k$ . In this case, the immersion of the matrix in the 75:25 medium led to the second step became practically negligible due to the rapid release of the active compound. On the other hand, the increase in the water proportion caused a higher swelling of the hydrophilic matrix based on PVA, and hence this phenomenon and the diffusion were the main mechanisms that drove the release process with  $k > k_b$ .

#### 4. Conclusions

The electrospinning technique demonstrated to be an efficient method to obtain fibrous nanostructures at a micro and nanometric scale. From the analysis of the rheological behavior of the solutions based on PVA, it emerged that the formulation of composite systems obtained assembling a PVA solution with a crosslinked emulsion modified the system viscosity, influencing the morphology of the obtained nanostructures. New ways of assembly active compounds into the system through electrospinning technique were performed, allowing the encapsulation of cabreuva EO through the combination of two-step emulsification and ionic gelation processes. The encapsulation of cabreuva EO was an effective strategy to achieve the sustained EO release by tuning the solution composition.

The electrospun fibers based on PVA and CH played a role as a vehicle for the controlled release of the cabreuva EO and demonstrated to have antimicrobial activities against broad spectra of micro-organisms (*Candida albicans*, *E. coli*, *S. aureus*, and *S. epidermidis*). Therefore, the active compound-loaded PVA nanofibers have great potential to be used as the delivery matrix in the near future.

Considering the obtained results, the encapsulation of the essential oil coupled with electrospinning technique constitutes an effective method for active compound delivery and could further help to achieve the sustained cabreuva essential oil release. Hence, the developed nanostructures would be materials with potential applications in the biomedical field in the form of wound care dressing.

**Figure captions**

**Figure 1.** BackScattering profiles (%) of the different emulsions: **a)** E1 (SDS 0.5 g l<sup>-1</sup>); **b)** E2 (CH / SDS 0.5g l<sup>-1</sup>); **c)** E3 (SDS 1 g l<sup>-1</sup>), and **d)** E4 (CH / SDS 1 g l<sup>-1</sup>). The arrow indicates the evolution over time from t = 0 to more than 8 days.

**Figure 2. a)** Particle size of formulated emulsions. Images obtained by TEM of the different emulsions: **b)** E1 (SDS 0.5 g l<sup>-1</sup>); **c)** E2 (CH / SDS 0.5 g l<sup>-1</sup>); **d)** E3 (SDS 1 g l<sup>-1</sup>), **e)** E4 (CH / SDS 1 g l<sup>-1</sup>) and, **f)** CE (CH / SDS 1 g l<sup>-1</sup>) cross-linked with sodium citrate.

**Figure 3.** SEM micrographs of electrospun nanofibers obtained by using PVA solutions: **a)** PVA 12%, **b)** PVA<sub>E</sub>, and **c)** (PVA+CE)<sub>E</sub> with their respectful fiber size distributions.

**Figure 4.** CLSM micrograph of (PVA + CE)<sub>E</sub> fibers obtained by electrospinning showing the distribution of cabreuva essential oil (*Myrocarpus fastigiatus*).

**Figure 5.** X-ray diffractograms of electrospun matrices based on PVA.

**Figure 6. a)** Thermogravimetric analysis curves of different tested samples obtained by electrospinning of PVA without and with crosslinked emulsion (CE), **b)** thermograms corresponding to the second stage of heating of the electrospun nanofibers of PVA without and with CE.

**Figure 7.** ATR-FTIR absorption spectra of cabreuva essential oil (*Myrocarpus fastigiatus*) and electrospun samples PVAE and (PVA+CE)<sub>E</sub>.

**Figure 8.** Controlled release of cabreuva essential oil in different ethanol: water media: 25:75 (blue color), 50:50 (dark cyan color), and 75:25 (green color). Data are the mean ± S.D. of four repetitions (n=4). **References:** Full-color symbol: experimental data, Black dash-dot-dot line: Gallagher-Corrigan model

**References**

- [1] M. Noruzi, Electrospun nanofibres in agriculture and the food industry: a review, *J. Sci. Food Agr.* 96(14) (2016) 4663-4678. <https://doi.org/10.1002/jsfa.7737>
- [2] J. Hu, J. Wei, W. Liu, Y. Chen, Preparation and characterization of electrospun PLGA/gelatin nanofibers as a drug delivery system by emulsion electrospinning, *J. Biomater. Sci. Polym. Ed.* 24(8) (2013) 972-985. <https://doi.org/10.1080/09205063.2012.728193>
- [3] S. Sapru, S. Das, M. Mandal, A. K. Ghosh, S. C. Kundu, Prospects of nonmulberry silk protein sericin-based nanofibrous matrices for wound healing—in vitro and in vivo investigations, *Acta Biomater.* 78 (2018)137-150. <https://doi.org/10.1016/j.actbio.2018.07.047>
- [4] P. Wen, M.H. Zong, R.J. Linhardt, K., Feng, H. Wu, Electrospinning: A novel nano-encapsulation approach for bioactive compounds, *Trends Food Sci. Technol.* 70 (2017) 56-68. <https://doi.org/10.1016/j.tifs.2017.10.009>
- [5] P.C. Caracciolo, F. Buffa, V. Thomas, Y.K. Vohra, G.A. Abraham, Biodegradable polyurethanes: comparative study of electrospun scaffolds and films, *J. Appl. Polym. Sci.* 121(6) (2011) 3292-3299. <https://doi.org/10.1002/app.33855>
- [6] B. Melendez-Rodriguez, K.J. Figueroa-Lopez, A. Bernardos, R. Martínez-Máñez, L. Cabedo, S. Torres-Giner, J.M. Lagaron, Electrospun antimicrobial films of poly (3-hydroxybutyrate-co-3-hydroxyvalerate) containing eugenol essential oil encapsulated in mesoporous silica nanoparticles, *Nanomaterials* 9(2) (2019) 227. <https://doi.org/10.3390/nano9020227>
- [7] M. Ranjbar-Mohammadi, S. Kargozar, S. H. Bahrami, M. T. Joghataei, Fabrication of curcumin-loaded gum tragacanth/poly (vinyl alcohol) nanofibers with optimized electrospinning parameters, *J. Ind. Textil.* 46(5) (2017) 1170-1192. <https://doi.org/10.1177/1528083715613631>
- [8] P. Puttamayutanon, K. Sutjarittangtham, S. Eitssayeam, P. Chantawannakul, Nanofiber production using polyvinylalcohol (PVA) and Thai honey and its properties, *In Adv. Mats. Res.* 506 (2012) 541-544. <https://doi.org/10.4028/www.scientific.net/AMR.506.541>
- [9] D.L. Custódio, V.F. Veiga-Junior, True and common balsams, *Rev. Bras. Farmacogn.* 22(6) (2012) 1372-1383. <http://dx.doi.org/10.1590/S0102-695X2012005000097>

- [10] X. H. Qin, S. Y. Wang, Electrospun nanofibers from crosslinked poly (vinyl alcohol) and its filtration efficiency, *J. App. Polym. Sci.* 109(2) (2008) 951-956. <https://doi.org/10.1002/app.28003>
- [11] R. Yoksan, J. Jirawutthiwongchai, K.Arpo, Encapsulation of ascorbyl palmitate in chitosan nanoparticles by oil-in-water emulsion and ionic gelation processes, *Colloids Surf. B Biointerfaces* 76(1) (2010), 292-297. <https://doi.org/10.1016/j.colsurfb.2009.11.007>
- [12] M. Angeles, H. L. Cheng, S. S. Velankar, Emulsion electrospinning: composite fibers from drop breakup during electrospinning, *Polym. Advan. Technol.* 19(7) (2008) 728-733. <https://doi.org/10.1002/pat.1031>
- [13] S. Mun, E. A. Decker, D. J. McClements, Influence of droplet characteristics on the formation of oil-in-water emulsions stabilized by surfactant– chitosan layers, *Langmuir* 21(14), (2005), 6228-6234. <https://doi.org/10.1021/la050502w>
- [14] H.X. Qi, P. Hu, J. Xu, A.J. Wang, Encapsulation of drug reservoirs in fibers by emulsion electrospinning: morphology characterization and preliminary release assessment. *Biomacromolecules* 7 (2006) 2327. <https://doi.org/10.1021/bm060264z>
- [15] F. Li, J. Li, X. Wen, S. Zhou, X. Tong, P. Su, H. Li, D. Shi, Anti-tumor activity of paclitaxel-loaded chitosan nanoparticles: An in vitro study, *Mat. Sci. Eng. C* 29(8) (2009) 2392-2397. <https://doi.org/10.1016/j.msec.2009.07.001>
- [16] J. Lamarra, S. Rivero, A Pinotti, Design of chitosan-based nanoparticles functionalized with gallic acid, *Mat. Sci. Eng. C* 67 (2016) 717-726. <https://doi.org/10.1016/j.msec.2016.05.072>
- [17] S. Villarruel, L. Giannuzzi, S. Rivero, A. Pinotti, Changes induced by UV radiation in the presence of sodium benzoate in films formulated with polyvinyl alcohol and carboxymethyl cellulose, *Mat. Sci. Eng. C* 56 (2015) 545-554. <https://doi.org/10.1016/j.msec.2015.07.003>
- [18] T. Tadros, Viscoelastic properties of sterically stabilised emulsions and their stability. *Adv. Colloid Interface Sci.* 222 (2015) 692-708. <https://doi.org/10.1016/j.cis.2015.03.001>
- [19] P. Sunintaboon, K. Pumduang, T. Vongsetskul, P. Pittayanurak, N. Anantachoke, P. Tuchinda, A. Durand, One-step preparation of chitosan/sodium dodecyl sulfate-stabilized oil-in-water emulsion of Zingiber cassumunar Roxb. oil extract, *Colloid. Surf. A Physicochem. Eng. Asp.* 414 (2012) 151-159. <https://doi.org/10.1016/j.colsurfa.2012.07.031>

- [20] S. Chatterjee, F. Salaün, C. Campagne, S. Vaupre, A. Beirão, A. El-Achari, Synthesis and characterization of chitosan droplet particles by ionic gelation and phase coacervation, *Polym. Bull.* 71(4) (2014) 1001-1013. <https://doi.org/10.1007/s00289-014-1107-4>
- [21] L. M. Julio, C. N. Copado, B. W. Diehl, V. Y. Ixtaina, M. C. Tomás, Chia bilayer emulsions with modified sunflower lecithins and chitosan as delivery systems of omega-3 fatty acids. *LWT* 89 (2018) 581-590. <https://doi.org/10.1016/j.lwt.2017.11.044>
- [22] N.S. Stamkulov, K.B. Mussabekov, S.B. Aidarova, P.F. Luckham, Stabilisation of emulsions by using a combination of an oil soluble ionic surfactant and water soluble polyelectrolytes. I: Emulsion stabilization and Interfacial tension measurements. *Colloid. Surf. A: Physicochem. Eng. Asp.* 335(1-3) (2009) 103-106. <https://doi.org/10.1016/j.colsurfa.2008.10.051>
- [23] H.D. Silva, M.A. Cerqueira, A.A. Vicente, Influence of surfactant and processing conditions in the stability of oil-in-water nanoemulsions, *J. Food Eng.* 167 (2015) 89-98. <https://doi.org/10.1016/j.jfoodeng.2015.07.037>
- [24] Z. Hou, Y. Gao, F. Yuan, Y. Liu, C. Li, D. Xu, Investigation into the physicochemical stability and rheological properties of  $\beta$ -carotene emulsion stabilized by soybean soluble polysaccharides and chitosan, *J. Agr. Food Chem.* 58(15) (2010) 8604-8611. <https://doi.org/10.1021/jf1015686>
- [25] T. Aoki, E. A. Decker, D. J. McClements, Influence of environmental stresses on stability of O/W emulsions containing droplets stabilized by multilayered membranes produced by a layer-by-layer electrostatic deposition technique, *Food Hydrocolloid.* 19(2) (2005) 209-220. <https://doi.org/10.1016/j.foodhyd.2004.05.006>
- [26] L. Di Giorgio, P.R. Salgado, A.N. Mauri, Encapsulation of fish oil in soybean protein particles by emulsification and spray drying, *Food Hydrocolloid.* 87 (2019) 891-901. <https://doi.org/10.1016/j.foodhyd.2018.09.024>
- [27] J. Pal, D. Wu, M. Hakkarainen, R. K. Srivastava, The viscoelastic interaction between dispersed and continuous phase of PCL/HA-PVA oil-in-water emulsion uncovers the theoretical and experimental basis for fiber formation during emulsion electrospinning, *Eur. Polym. J.* 96 (2017) 44-54. <https://doi.org/10.1016/j.eurpolymj.2017.09.004>



- [28] T. Phachamud, M. Phiriyawirut, Physical properties of polyvinyl alcohol electrospun fiber mat, *Res. J. Pharm. Biol. Chem. Sci.*, 2 (2011) 675-684. ISSN: 0975-8585
- [29] A. Pangon, S. Saesoo, N. Saengkrit, U. Ruktanonchai, V. Intasanta, Multicarboxylic acids as environment-friendly solvents and in situ crosslinkers for chitosan/PVA nanofibers with tunable physicochemical properties and biocompatibility, *Carbohydr. Polym.* 138 (2016) 156-165. <https://doi.org/10.1016/j.carbpol.2015.11.039>
- [30] S. Talebian, A.M. Afifi, H.M. Khanlou, Fabrication and characterisation of chitosan/poly vinyl alcohol nanofibres via electrospinning, *Mater. Res. Innov.* 18(6) (2014) S6-331. <https://doi.org/10.1179/1432891714Z.000000000979>
- [31] K. A. Rieger, J. D. Schiffman, Electrospinning an essential oil: Cinnamaldehyde enhances the antimicrobial efficacy of chitosan/poly (ethylene oxide) nanofibers, *Carbohydr. Polym.* 113 (2014) 561-568. <https://doi.org/10.1016/j.carbpol.2014.06.075>
- [32] A. López-Córdoba, G. R. Castro, S. Goyanes, A simple green route to obtain poly (vinyl alcohol) electrospun mats with improved water stability for use as potential carriers of drugs, *Mats. Sci. Eng. C* 69 (2016) 726-732. <https://doi.org/10.1016/j.msec.2016.07.058>
- [33] Hong, K.H., Preparation and properties of polyvinyl alcohol/tannic acid composite film for topical treatment application, *Fibers Pol.* 17(12) (2016) 1963-1968. <https://doi.org/10.1007/s12221-016-6886-9>
- [34] R. Y. Basha, T. S. Sampath Kumar, M. Doble, Electrospun nanofibers of curdlan ( $\beta$ -1, 3 Glucan) blend as a potential skin scaffold material, *Macromol. Mater. Eng.* 302(4) (2017) 1600417. <https://doi.org/10.1002/mame.201600417>
- [35] M. S. Enayati, T. Behzad, P. Sajkiewicz, R. Bagheri, L. Ghasemi-Mobarakeh, W. Łojkowski, Z. Pahlevanneshan, M. Ahmadi, Crystallinity study of electrospun poly (vinyl alcohol) nanofibers: effect of electrospinning, filler incorporation, and heat treatment, *Iran. Polym. J.* 25(7) (2016) 647-659. <https://doi.org/10.1007/s13726-016-0455-3>
- [36] M. Krstić, M. Radojević, D. Stojanović, V. Radojević, P. Uskoković, S. Ibrić, Formulation and characterization of nanofibers and films with carvedilol prepared by electrospinning and solution casting method, *Eur. J. Pharm. Sci.* 101 (2017) 160-166. <https://doi.org/10.1016/j.ejps.2017.02.006>

- [37] E. A. Van Etten, E. S. Ximenes, L. T. Tarasconi, I. T. Garcia, M. M. Forte, H. Boudinov, Insulating characteristics of polyvinyl alcohol for integrated electronics, *Thin Solid Films* 568 (2014) 111-116. <https://doi.org/10.1016/j.tsf.2014.07.051>
- [38] O. Olabisi, L. M. Robeson, M. T. Shaw, *Polymer-Polymer Miscibility*, 1979.
- [39] L. Deng, X. Kang, Y. Liu, F. Feng, H. Zhang, Characterization of gelatin/zein films fabricated by electrospinning vs solvent casting, *Food Hydrocolloid.* 74 (2018) 324-332. <https://doi.org/10.1016/j.foodhyd.2017.08.023>
- [40] H. Adeli, M. T. Khorasani, M. Parvazinia, Wound dressing based on electrospun PVA/chitosan/starch nanofibrous mats: Fabrication, antibacterial and cytocompatibility evaluation and in vitro healing assay, *Int. J. Biol. Macromol.* 122 (2019) 238-254. <https://doi.org/10.1016/j.ijbiomac.2018.10.115>
- [41] P. Zahedi, M. Fallah-Darrehchi, Electrospun egg albumin-PVA nanofibers containing tetracycline hydrochloride: Morphological, drug release, antibacterial, thermal and mechanical properties, *Fiber. Polym.* 16(10) (2015) 2184-2192. <https://doi.org/10.1007/s12221-015-5457-9>
- [42] M.P. Sanches, I.P. Gross, R.H. Saatkamp, A.L. Parizea, V. Soldi, Chitosan-sodium alginate polyelectrolyte complex coating Pluronic® F127 nanoparticles loaded with citronella essential oil, *J. Braz. Chem. Soc.*, 31(4) (2020) 803-812. <http://dx.doi.org/10.21577/0103-5053.20190244>
- [43] R. W. Kormsmeier, R. Gurny, E. Doelker, P. Buri, N. A. Peppas, Mechanisms of solute release from porous hydrophilic polymers, *Int. J. Pharm.* 15(1) (1983) 25-35. [https://doi.org/10.1016/0378-5173\(83\)90064-9](https://doi.org/10.1016/0378-5173(83)90064-9)
- [44] S. Estevez-Areco, L. Guz, R. Candal, S. Goyanes, Release kinetics of rosemary (*Rosmarinus officinalis*) polyphenols from polyvinyl alcohol (PVA) electrospun nanofibers in several food stimulants, *Food Packag. Shelf Life.* 18 (2018) 42-50. <https://doi.org/10.1016/j.fpsl.2018.08.006>
- [45] J. Villasante, E. Codina, G. I. Hidalgo, A. Martínez de Ilarduya, S. Muñoz-Guerra, M. P. Almajano, Poly ( $\alpha$ -Dodecyl  $\gamma$ -Glutamate)(PAAG-12) and polylactic acid films charged with  $\alpha$ -

- Tocopherol and their antioxidant capacity in food models, *Antioxidants* 8(8) (2019) 284.  
<http://dx.doi.org/10.3390/antiox8080284>
- [46] A. M. Moydeen, M.S.A., Padusha, E.F. Aboelfetoh, S.S. Al-Deyab, M.H. El-Newehy, Fabrication of electrospun poly (vinyl alcohol)/dextran nanofibers via emulsion process as drug delivery system: Kinetics and in vitro release study, *Int. J. Biol. Macromol.* 116 (2018) 1250-1259. <https://doi.org/10.1016/j.ijbiomac.2018.05.130>
- [47] M. A. Souza, J. E. Oliveira, E. S. Medeiros, G. M. Glenn, L. H. Mattoso, Controlled release of linalool using nanofibrous membranes of poly (lactic acid) obtained by electrospinning and solution blow spinning: a comparative study, *J. Nanosci. Nanotechnol.* 15(8) (2015) 5628-5636. <https://doi.org/10.1166/jnn.2015.9692>
- [48] J. Lamarra, L. Giannuzzi, S. Rivero, A Pinotti, Assembly of chitosan support matrix with gallic acid-functionalized nanoparticles, *Mat. Sci. Eng. C* 79 (2017) 848-859.  
<http://dx.doi.org/10.1016/j.msec.2017.05.104>
- [49] A. Faidi, M.A. Lassoued, M.E. Becheikh, M. Touati, J.F. Stumbé, F. Farhat, Application of sodium alginate extracted from a Tunisian brown algae *Padina pavonica* for essential oil encapsulation: Microspheres preparation, characterization and in vitro release study. *Int. J. Biol. Macromol.* 136 (2019) 386-394. <https://doi.org/10.1016/j.ijbiomac.2019.06.023>
- [50] F.F. da Costa, E.S Araújo, M.L. Nascimento, H.P. de Oliveira, Electrospun fibers of enteric polymer for controlled drug delivery, *Int. J. Polym. Sci.* 2015 (2015) 1-8.  
<http://dx.doi.org/10.1155/2015/902365>
- [51] A. Rezaei, A. Nasirpour, Evaluation of release kinetics and mechanisms of curcumin and curcumin- $\beta$ -cyclodextrin inclusion complex incorporated in electrospun almond Gum/PVA nanofibers in simulated saliva and simulated gastrointestinal conditions. *BioNanoSci.* 9(2) (2019) 438-445. <https://doi.org/10.1007/s12668-019-00620-4>

### Author's contributions

J.L.: Methodology, validation, investigation. M.N.C.: Investigation. S.R.: Writing-original draft, Writing-review & editing. A.P.: Writing-original draft, Writing-review & editing, Funding acquisition. All authors have approved the final version of the

Journal Pre-proof

### **Conflict of interest**

The authors declare that they have no conflicts of interest.

### **Acknowledgments**

This work was supported by the Argentinean Agency for the Scientific and Technological Promotion (ANPCyT) (Project PICT 2016-0504). The authors thank Eng. Dario Crottogini and Eng. Jorge Crottogini, Esencias del Bosque, for providing cabreuva essential oil.

**Table 1.** Components of formulated emulsions; zeta potential values (ZP) and reduction in *BackScattering* (BS) for the different emulsions tested after seven days

Emulsion	Concentration				ZP (mV) <sup>*</sup>	BS reduction (%)
	CH (% w/v)	PVA (% w/v)	SDS (g l <sup>-1</sup> )	EO (% v/v)		
E <sub>1</sub>	-	0.75	0.5	7.5	-9.1 (1.4) <sup>a</sup>	61.2 <sup>d</sup>
Lamarra <i>et al.</i> Table 1		0.75	0.5	7.5	65.8 (0.7) <sup>b</sup>	15.8 <sup>b</sup>
E <sub>3</sub>	-	0.75	1	7.5	-40.6 (0.4) <sup>c</sup>	48.7 <sup>c</sup>
E <sub>4</sub>	0.75	0.75	1	7.5	74.8 (4.0) <sup>d</sup>	6.13 <sup>a</sup>

<sup>\*</sup> Different letters within the same column indicate significant differences between the samples (p < 0.05)

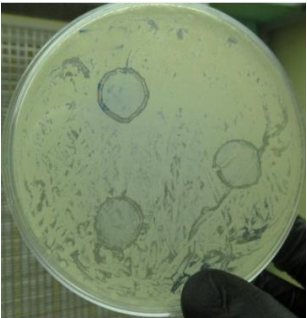
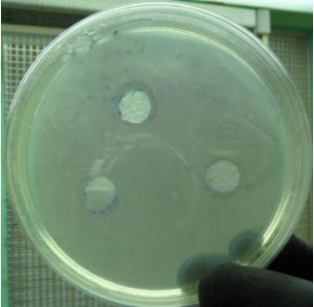
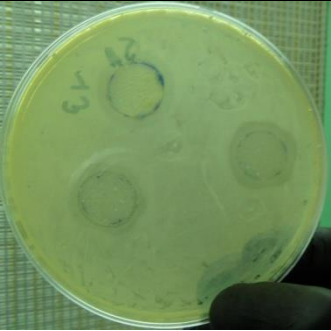

**Table 2.** Fitting parameters of the Ostwald de Waele model and apparent viscosity determined at  $500 \text{ s}^{-1}$  of the crosslinked emulsion (CE), PVA 14% and (PVA+CE)

Sample*	$k_v$	$n_v$	$\eta$ (Pa.s) ( $500 \text{ s}^{-1}$ )
CE	-	1.0 ( 0.1 ) <sup>c,*</sup>	0.0093 (0.002) <sup>a</sup>
<sup>a</sup> PVA	24.27(0.08) <sup>a</sup>	0.649 (0.002) <sup>a</sup>	2.69 (0.03) <sup>c</sup>
<sup>a</sup> PVA+CE	5.1 (0.1) <sup>b</sup>	0.820 (0.003) <sup>b</sup>	1.68 (0.07) <sup>b</sup>

<sup>a</sup>The values reported correspond to the upward ramp of the flow behavior curve

\* Different letters within the same column indicate significant differences between the samples ( $p < 0.05$ )

**Table 3.** Antimicrobial capacity of electrospun nanofibers (PVA+CE)<sub>E</sub> against inocula of  $10^7$ - $10^8$  CFU ml<sup>-1</sup> of different microorganisms

<i>Patogen</i>	<i>Inhibition halo (cm)</i>	<i>Picture</i>
Candida albicans	1.9 (0.07) <sup>a,b</sup>	
Escherichia coli	1.6 (0.06) <sup>a</sup>	
Staphylococcus aureus	2.1 (0.09) <sup>b</sup>	
Staphylococcus epidermidis	1.8 (0.10) <sup>a,b</sup>	

\* Different letters within the same column indicate significant differences between the samples (p < 0.05)



**Table 4.** Parameters obtained from the Korsmeyer-Peppas, Gallagher-Corrigan, Gompertz, Weibull, and Higuchi models for controlled release of cabreuva essential oil in media with different ethanol: water ratios

#Release medium	Korsmeyer-Peppas (Eq.2)			Gallagher-Corrigan (Eq. 3)			Gompertz (Eq. 4)			Weibull (Eq. 5)			Higuchi (Eq. 6)	
	n	k (min <sup>-1</sup> )	R <sup>2</sup>	K <sub>b</sub> (h <sup>-1</sup> )	k	R <sup>2</sup>	a	b	R <sup>2</sup>	a	b	R <sup>2</sup>	a	R <sup>2</sup>
25:75	0.37	0.013	0.965	0.086	2.13	0.986	2.10	0.61	0.968	7.72	0.46	0.938	0.10	0.908
50:50	0.65	0.010	0.997	0.255	2.64	0.999	1.69	0.73	0.979	5.21	0.48	0.953	0.14	0.912
75:25	1.0	0.059	0.930	4.726	0.009	0.971	0.19	1.53	0.950	0.45	0.67	0.897	*na	na

#Release medium: ethanol: water

\*na: not applicable

## Highlights

Cabreuva essential oil (EO) emulsions were included in a PVA electrospun matrix

Electrospun active matrix was effective against a broad spectrum of microorganisms

Electrospun nanostructure demonstrated capacity to control the cabreuva EO release

Electrospun nanostructure could be applied as topical dressings in biomedical field

Journal Pre-proof

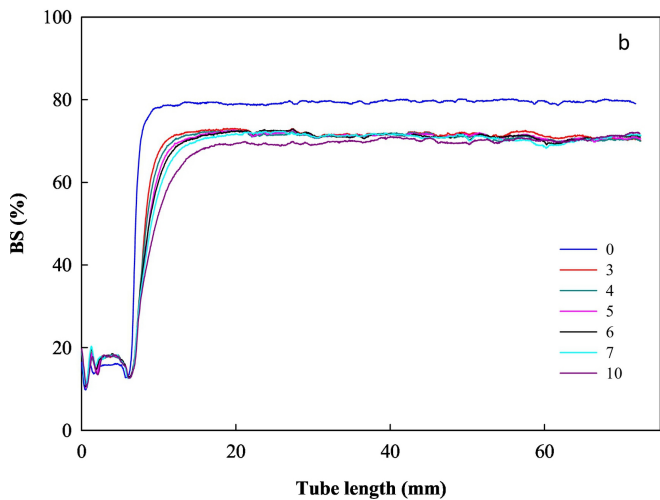
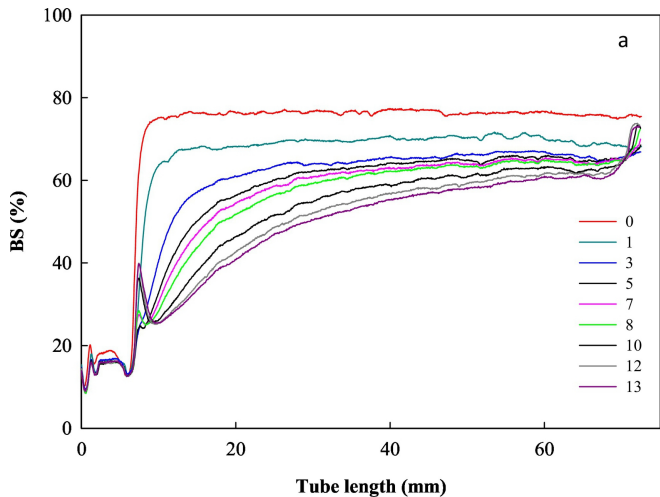


Figure 1r1

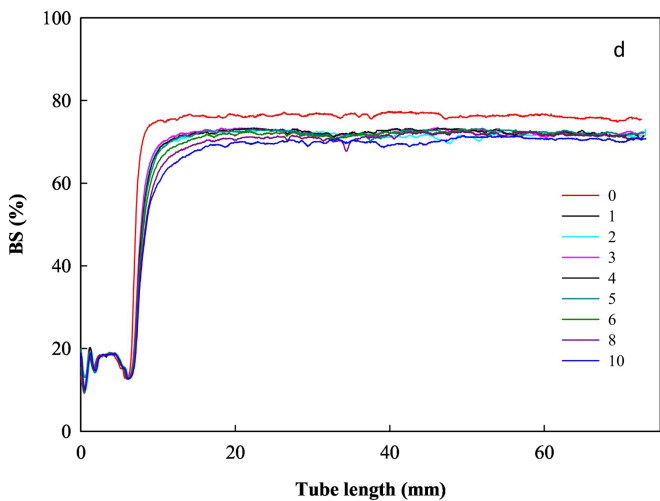
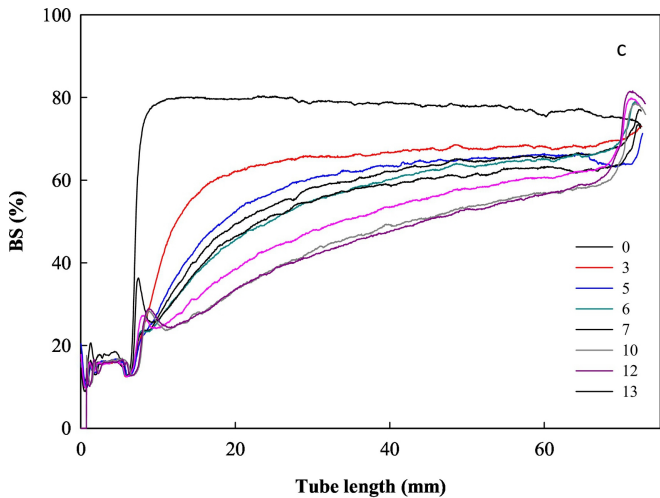


Figure 1r2

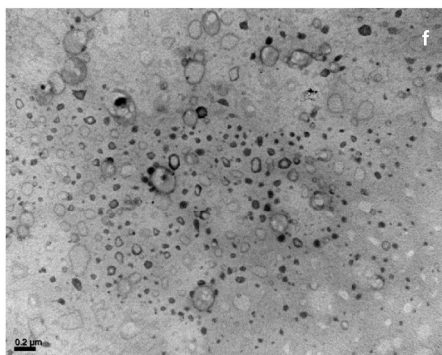
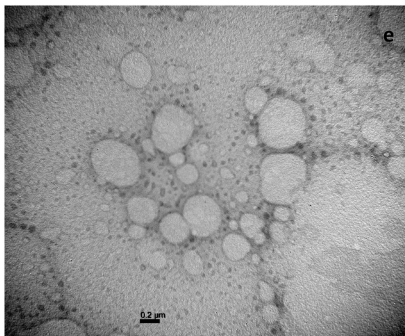
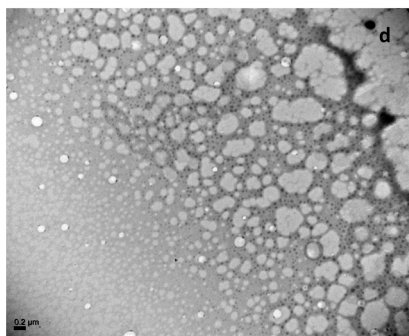
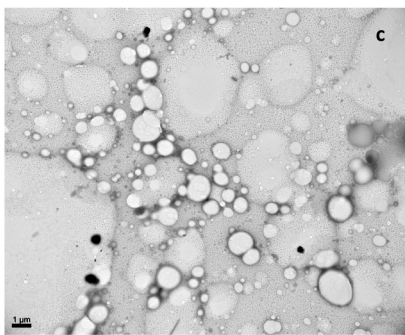
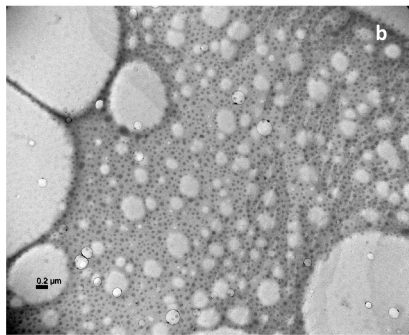
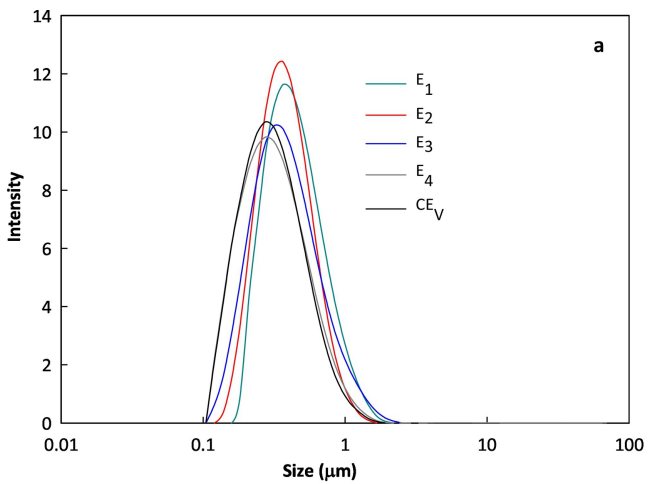


Figure 2

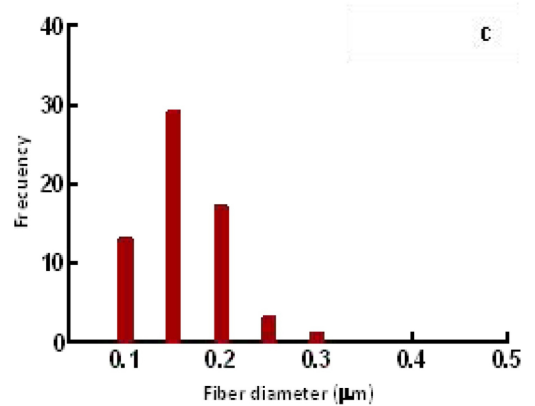
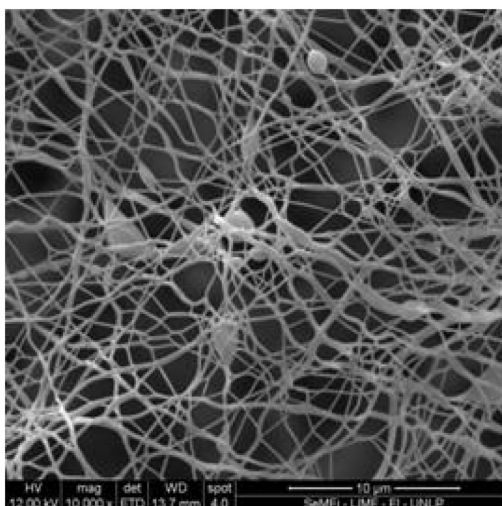
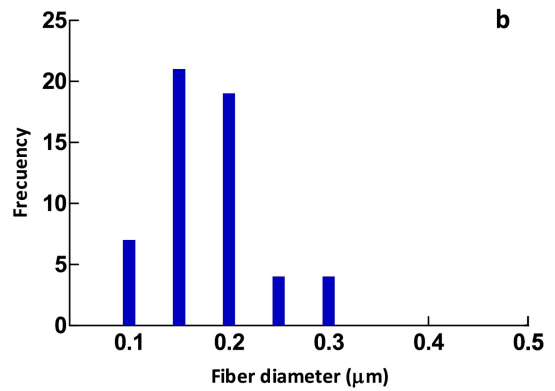
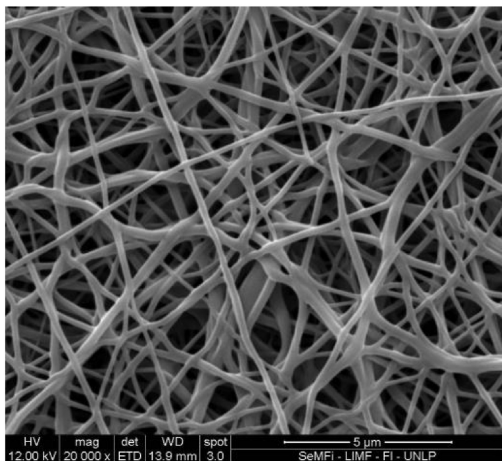
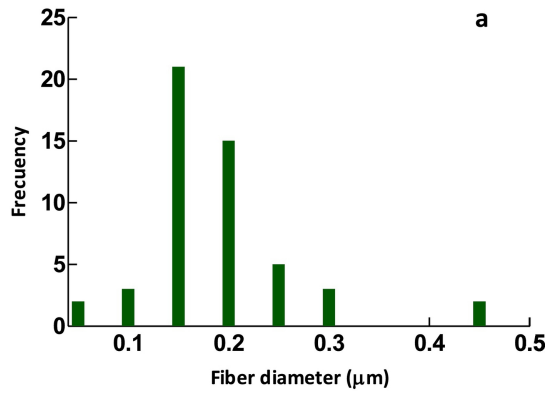
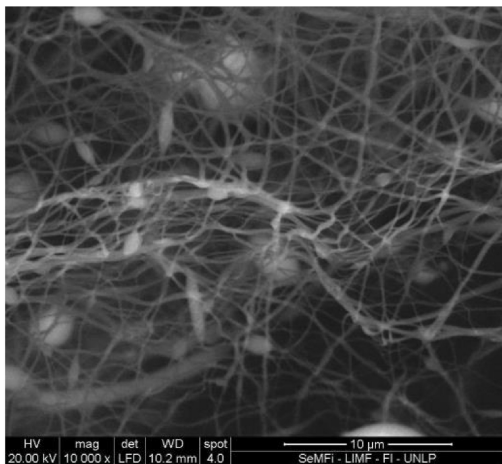
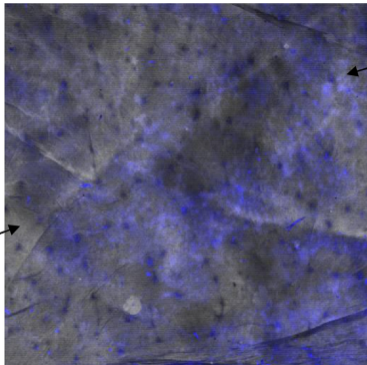


Figure 3

**Electrospun  
matrix**



**Cabreuva  
essential oil**



**Figure 4**

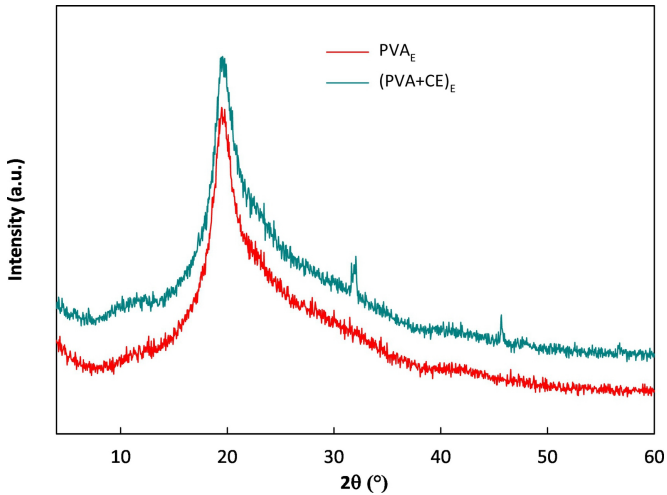


Figure 5



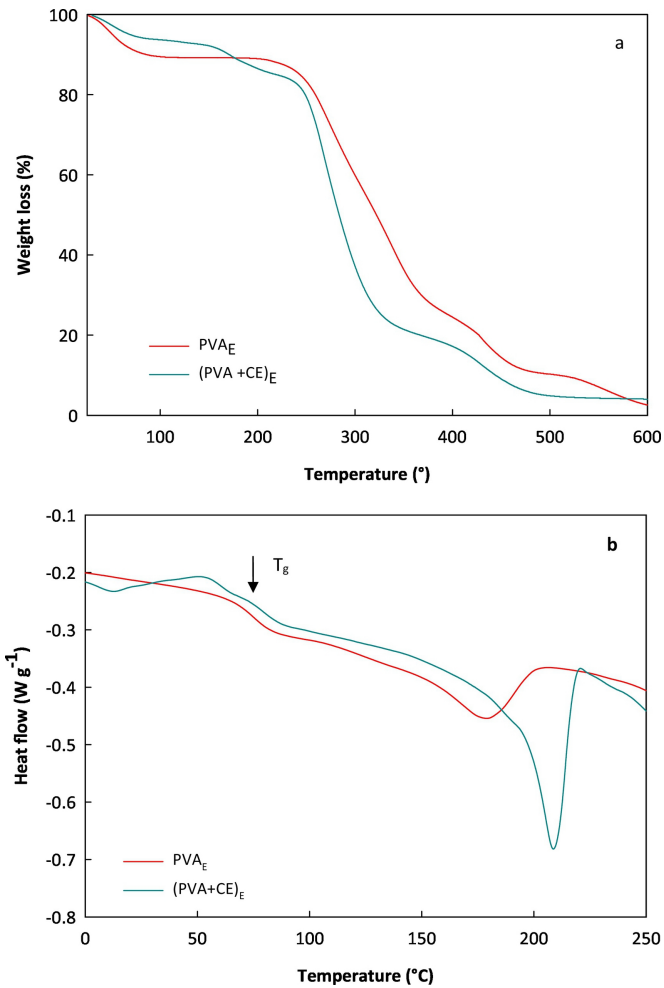


Figure 6

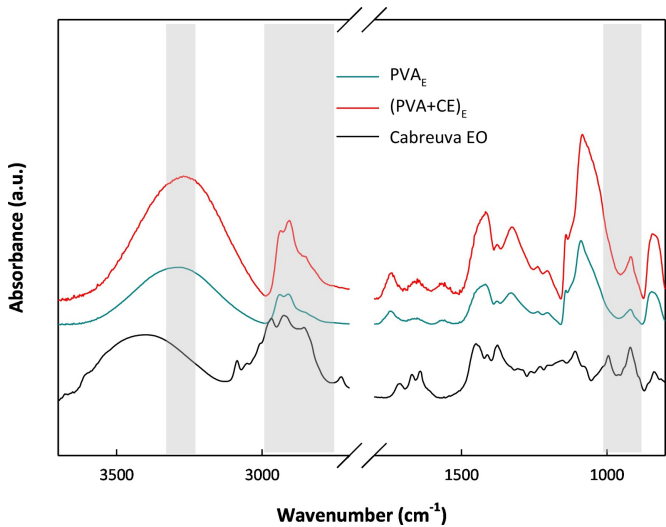


Figure 7

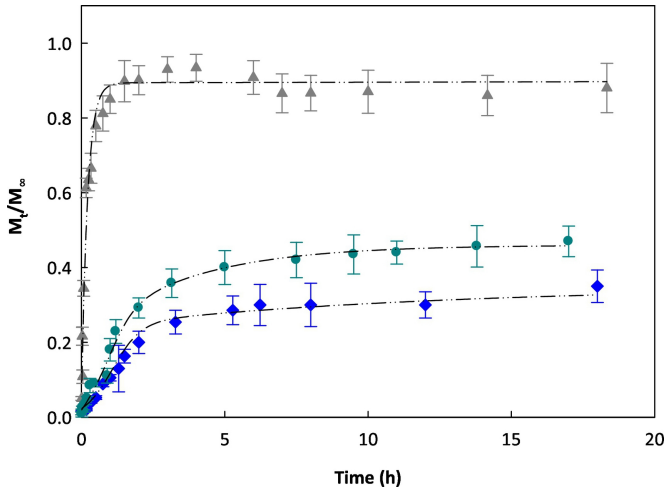


Figure 8